RESEARCH ARTICLE

Giant Crystalline Molecular Rotors that Operate in the Solid State

Rempei Ando,[b] Ayana Sato-Tomita,[c] Hajime Ito,*[a,b] and Mingoo Jin*[a]

[a] Prof. Dr. H. Ito (corresponding author), Prof. Dr. M. Jin (corresponding author),
Department Institute for Chemical Reaction Design and Discovery (WPI-ICReDD)
Institution Hokkaido University
Address 1 Sapporo, Hokkaido, 060-8628, Japan
E-mail: Mingoo Jin (mingoo@icredd.hokudai.ac.jp), Hajime Ito (hajito@eng.hokudai.ac.jp)

[b] R. Ando, Prof. Dr. H. Ito
Department Division of Applied Chemistry and Frontier Chemistry Center (FCC), Faculty of Engineering
Institution Hokkaido University
Address 1 Sapporo, Hokkaido, 060-8628, Japan

[c] Dr. A. Sato-Tomita
Department School of Medicine
Institution Jichi Medical University
Address 1 Shimotsuke-shi, Tochigi-ken, 329-0498, Japan

Supporting information for this article is given via a link at the end of the document.

Abstract: Molecular motion in the solid state is typically precluded by the highly dense environment, and only molecules with a limited range of sizes show such dynamics. Here, we demonstrate the solid-state rotational motion of two giant molecules, i.e., triptycene and pentiptycene, by encapsulating a bulky N-heterocyclic carbene (NHC) Au(I) complex in the crystalline media. To date, triptycene is the largest molecule (surface area: 245 Å^2; volume: 219 Å^3) for which rotation has been reported in the solid state, with the largest rotational diameter among reported solid-state molecular rotors (9.5 Å). However, the pentiptycene rotator that is the subject of this study (surface area: 392 Å^2; volume: 361 Å^3; rotational diameter: 13.0 Å) surpasses this record. Single-crystal X-ray diffraction analyses of both the developed rotors revealed that these possess sufficient free volume around the rotator. The molecular motion in the solid state was confirmed using variable-temperature solid-state ^{2}H spin-echo NMR studies. The triptycene rotor exhibited three-fold rotation, while temperature-dependent changes of the rotational angle were observed for the pentiptycene rotor.

Introduction

The rotational dynamics of large molecules with complicated three-dimensional structures such as proteins are ubiquitous in nature, and often play fundamental roles in living systems.[1-5] In artificial molecules, iptycenes, which are a class of aromatic compounds with arene units fused to a [2.2.2]bicyclooctatriene bridgehead system, have been widely used as key units for developing molecular motion and functional properties such as photo-functional, electronic, and molecular-assembly properties. In particular, triptycene and pentiptycene derivatives have found a wide range of applications based on their unique structures, which are characterized by three-dimensionally fused aromatic moieties and π-rich features (Figure 1a).[6-8] Generally, fluid phases allow molecular dynamics to occur, while solid phases are considered to be least suitable for the mechanical motion of large molecules. The difficulties associated with achieving molecular motion in the solid state are mostly due to the densely packed environment surrounding the molecules. Triptycene and pentiptycene have a large surface area and volume due to the multiple three-dimensionally fused arylene units, which results in the formation of intermolecular π–π or CH–π interactions that suppress the mechanical motion in the solid state (Figure 1b). However, design elements that generate sufficient volume around large molecules may allow for large angular displacements, even in the solid phase.

In the past two decades, molecular rotational motion in the solid state with functional properties has been intensely investigated using ‘amphidynamic crystals’, which exhibit fast molecular rotation with highly ordered structures in the solid phase (Figure 1c).[9-16] Amphidynamic crystals, whose physical properties can be controlled by altering the molecular rotation, represent a critical development in solid-state functional materials, as well as a promising strategy to transduce molecular-level functions to the macroscopic scale.[11,17-26] The blueprint for such crystalline materials involves two bulky stators linked to the rotator via an axis moiety. Gyroscope-like molecular rotors, dumbbell-shaped molecules, and porous materials such as metal–organic frameworks (MOFs) have been employed as the structural motifs.[10,12,13,15,16] In many cases, the molecular rotation has been achieved using phenylenes as rotators. However, the construction of crystalline molecular rotors that allow the rotation of large molecules with complex structures remains a significant challenge.

When the rotator size is increased compared to the typical phenylene unit in such systems, a larger rotational area is required in the solid state. In general, large local free volumes are unlikely to form during the crystallization process. Thus, it is difficult to design a large local free volume around such large rotators. Furthermore, large rotators have larger contact faces and multiple interactions in the crystal, which are unfavorable for achieving molecular motion. Garcia-Garibay et al. have succeeded in rotating triptycene in the solid state by using a dumbbell-shaped molecular design with a large, bulky, and

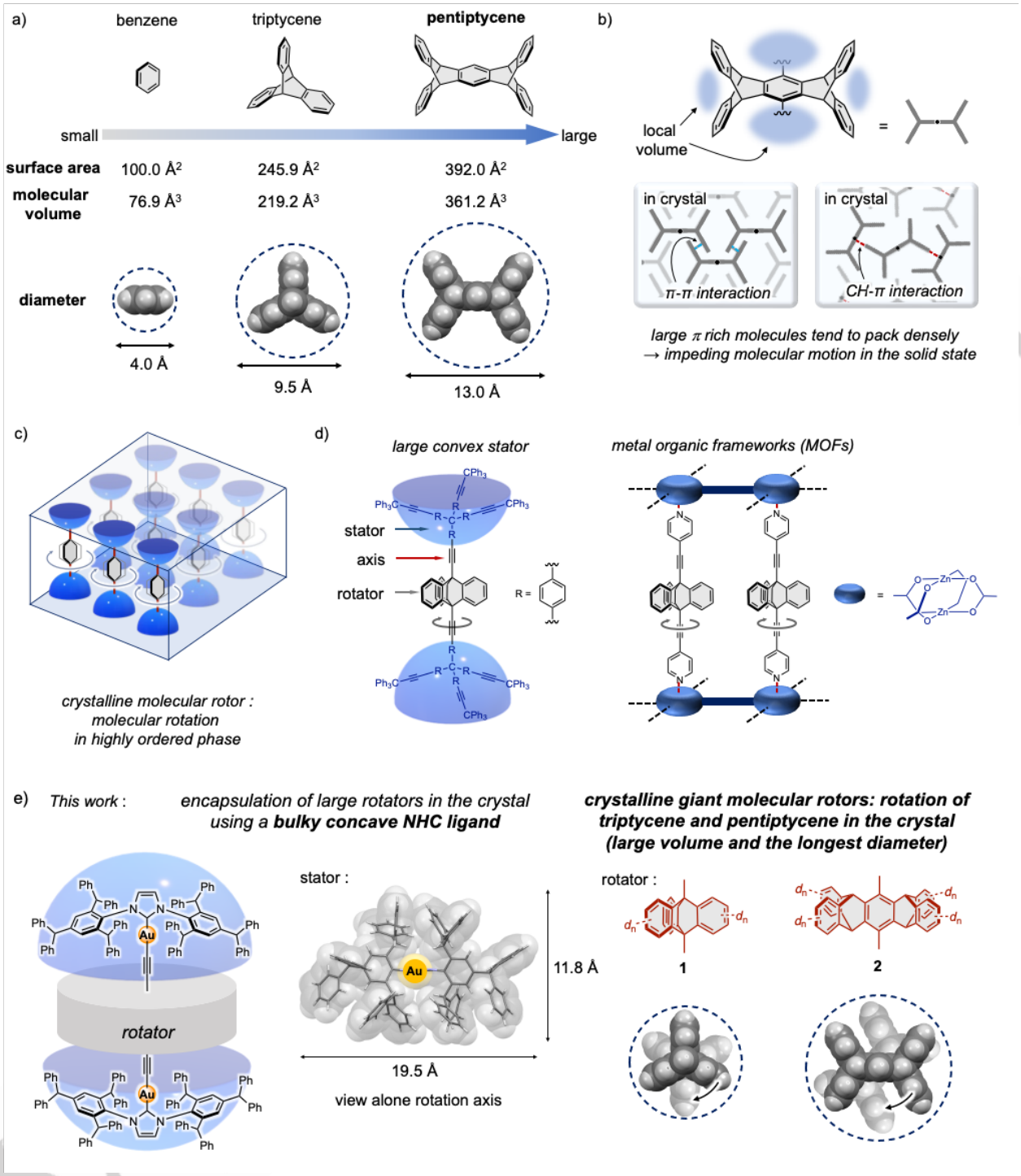

Figure 1. a) Comparison of the molecular size (surface, volume, and rotational diameter) of benzene, triptycene, and pentiptycene. b) Schematic illustration of the crystal-packing arrangement of pentiptycene. Multiple π–π and CH–π interactions are able to create form a dense crystal structure. c) Schematic illustration of a crystalline molecular rotor. d) Previously reported molecular rotors based on triptycene. e) Chemical structures of molecular rotors **1** and **2**. The area enclosed by the IPr# ligand is estimated to be 11.8 ×19.5 Å^2.

convex stator (Figure 1d).[27] Additionally, MOFs that bear a ligand in which a triptycene moiety is centrally introduced have been developed, and rotary motion of the triptycene moieties has been observed in the solid state (Figure 1d).[28] Recently, we have developed a new platform for crystalline molecular rotors using a concave *N*-heterocyclic carbene (NHC) metal complex as a stator to encapsulate the central rotator unit.[29,30] The main advantage of this approach is that the rotator moiety can be shielded from undesired intermolecular steric hinderance in crystalline media. Based on this feature, we envisioned that a larger and bulkier NHC ligand could be used to create a large rotational volume for the rotation of large rotators such as pentiptycene, having a larger volumn and surface area than that of triptycene, in crystals.

In order to realize this concept, we have designed the giant NHC–Au(I) complex molecular rotors **1** and **2** using the 1,3-bis(2,4,6-tri(diphenylmethyl))imidazo-2-ylidene (IPr#) ligand[31] as the concave bulky stator with triptycene and pentiptycene rotators, respectively, and observed rotational motion of these iptycene

derivatives in the crystalline state (Figure 1e). The IPr# ligand was introduced given its sterically highly demanding structure, which could prevent close rotator–rotator or rotator–ligand packing. Both crystalline rotors were characterized using single-crystal X-ray diffraction, which revealed that the bulky NHC ligand allows the construction of a loose packing environment near the rotators. ^{2}H spin-echo solid-state NMR measurements of the crystalline samples confirmed that rotational motion occurred in the crystals at temperatures above 293 K for rotor **1** and 233 K for rotor **2**.

Results and Discusson

Giant rotors **1** and **2** were synthesized from the corresponding deuterated diethynyl iptycene compounds owing to carry out the solid-state ^{2}H NMR measurement and IPr# Au(I) chloride using standard alkynation conditions (Scheme 1). Rotor **1** was obtained in 89% yield under moderate reaction conditions, while the synthesis of rotor **2** required high temperature during the reaction to achieve 49% yield. Rotor **1** was crystallized by solvent diffusion from a dichloromethane solution of **1** layered with hexane, yielding crystal $\mathbf{1}_{sol}$ (Scheme 2). For crystallizing rotor **2**, the vapor-diffusion method was used for a $CHCl_3$ solution of **2** that was exposed to Et_2O vapor. The crystallization of rotor **2** yielded two polymorphs (solvated and non-solvated crystals) in the same vial, as confirmed by single-crystal X-ray analysis (SC-XRD), described in Figure S1 and S2. The solvated crystal of rotor **2** (crystal $\mathbf{2}_{sol}$) was transformed into the non-solvated crystal **2** by exposing the crystal to reduced pressure (Figure S1–S3 and S8–S12, for details, see the Supporting Information). Rotors **1** and **2** were additionally characterized using ^{1}H and ^{13}C NMR spectroscopy, MS-EI-mass spectrometry, and elemental analysis.

SC-XRD measurements were performed to obtain precise structural information for giant rotor **1**, achieved by using crystal $\mathbf{1}_{sol}$. Rotor **1** crystallizes in the triclinic space group $P2_1/c$ with four molecules per unit cell (Z = 4) (Table S2). Moreover, molecules of hexane were found in the crystal structure, with a chemical occupancy of 0.5 (Figure 2a). The C–C distances between the phenylene groups of the NHC ligand and the triptycene moiety varied from 3.34 Å to 3.83 Å (Figure 2b). Although one of the C–C distance is shorter than the sum of the van-der Waals radii of the carbon atoms (3.4 Å), implying a potential π-π interaction, the remaining phenyl rings near the rotator are noticeably distanced, which suggests reduced steric hindrance between the NHC ligand and the rotor and thus a favorable packing manner for the molecular motion of triptycene (Figure S7). The packing environment around rotor **1** is shown in Figure 2c. The two phenyl groups highlighted in purple are close to the rotator. The distances between these phenylene moieties and the rotational axis of triptycene are approximately 5.59 and 5.91 Å, and thus longer than the rotational radius of triptycene (4.75 Å). This packing environment around the triptycene rotator indicates that the rotation of triptycene should be achievable. However, the presence of hexane near the rotator may sterically disturb the rotation of triptycene, even though the distance between hexane and the rotational center (4.86 Å) is greater than the rotational radius of triptycene. In order to promote the rotational motion of triptycene, the solvated crystal (crystal $\mathbf{1}_{sol}$) was exposed to

Scheme 1. Synthesis of giant rotors **1** and **2**

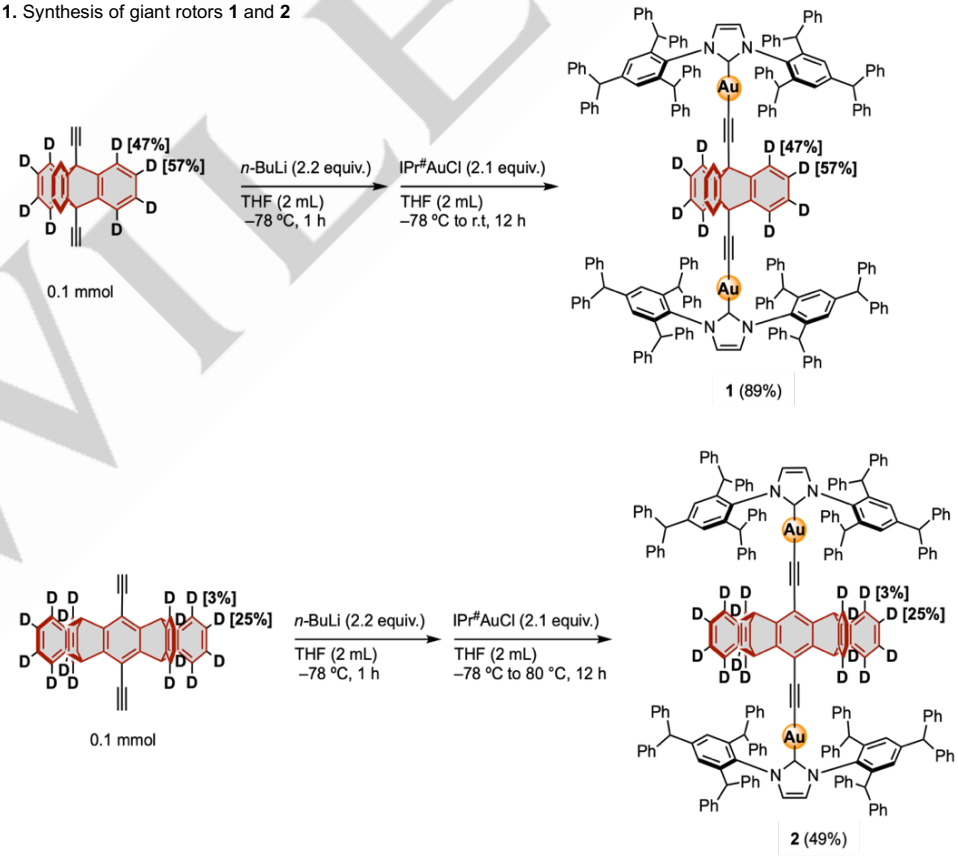

Scheme 2. Preparation of the crystalline samples of rotors **1** and **2**

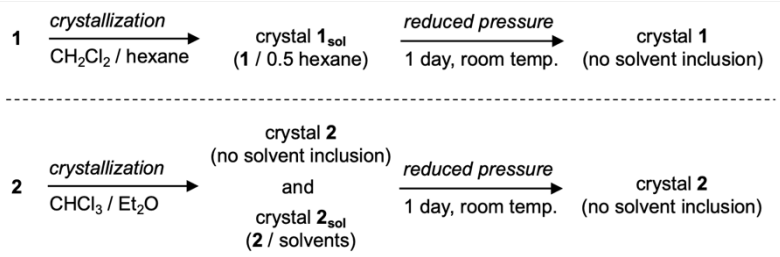

reduced pressure under room temperature for 1 day in order to remove hexane molecules near the rotators (Scheme 2), and complete desolvation was confirmed using TGA analysis (Figure S5). The obtained PXRD pattern has several identical main peaks to the pattern simulated using the SC-XRD data. Moreover, a simulation of the PXRD pattern using the *Whole Powder Pattern Fitting* (WPPF) method revealed that the indexed crystallographic parameters are almost identical to the SC-XRD data of crystal **1**$_{sol}$ (Figures S3–S4 and Table S1)**.** These indicated that no phase transition occurred during the desolvation and the crystallinity was maintained. In addition, the desolvated crystalline sample showed no thermally triggered martensic transitions, determined by variable-temperature PXRD measurements and a DSC study in the range 200 K–350 K (Figures S3a and S6). The obtained results suggest that the steric environment near the triptycene rotator of **1** can be expected to remain constant upon changing the temperature.

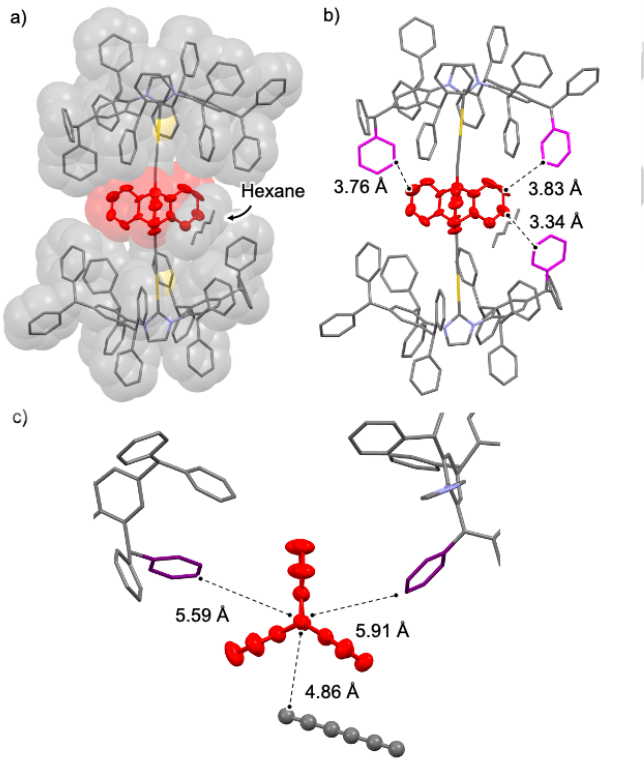

Figure 2. a) Structure of giant rotor **1** in crystal **1**$_{sol}$; b) several close C–C distances between the phenylene groups of the NHC moiety and triptycene. c) Packing geometry around the rotator; phenylene groups colored purple are close to the rotator.

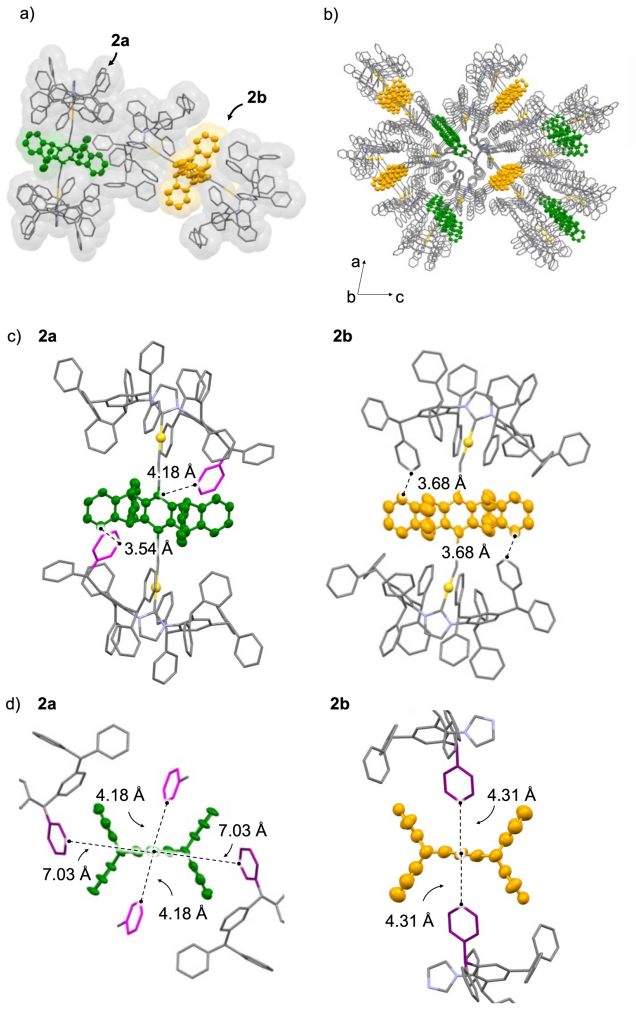

Figure 3. a) Structure of giant rotor **2** in crystal **2**; the two crystallographically independent rotors are denoted as rotor **2a** (green) and **2b** (orange). b) Crystal-packing arrangement of rotor **2**. c) Selected C–C distances between the phenylene groups of the NHC moiety and pentiptycene. d) Packing geometry around rotors **2a** and **2b** shown with distances relative to the rotational axis of the central pentiptycene (Au–C bond). Phenylene groups of the NHC ligand near of the rotators are colored purple.

An SC-XRD analysis of giant rotor **2** without solvent inclusion revealed two independent rotors (denoted as rotor **2a** and **2b**; shown in Figure 3 in green and orange, respectively) per unit cell ($Z = 2$), which packed in the space group *P*-1 (Figure 3a). The pentiptycene rotator is slightly bent relative to the two NHC units due to the flexibility of the alkyne axis. In terms of the molecular packing structure, rotors **2a** and **2b** align along the b-axis and form columnar structures (Figure 3b). Each pentiptycene

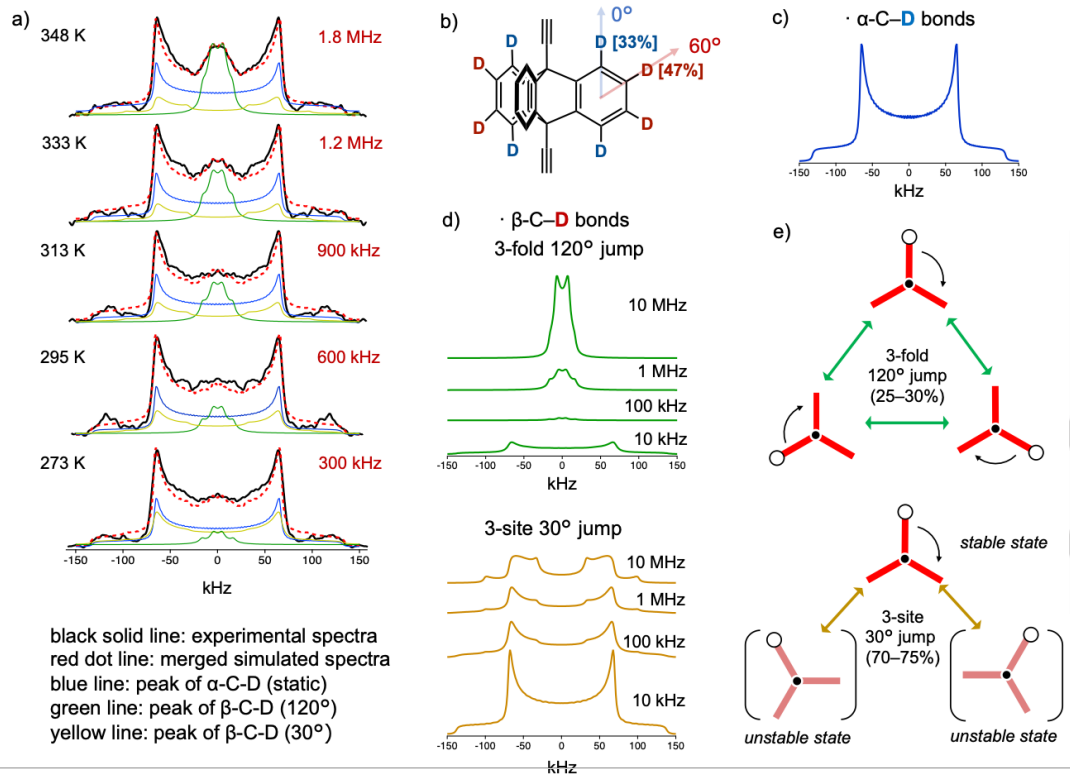

Figure 4. a) Variable-temperature (VT) solid-state (SS) ^{2}H NMR studies of rotor **1** in crystal **1**. Experimental SS NMR spectra (black lines) and simulated spectra: superposition of the simulated spectra (red dashed lines), static simulated spectra derived from the α-D position (blue solid lines), simulated spectrum for the 3-fold 120° jump (green solid lines), and simulated spectra for the 3-fold 30° jump derived the from β-D position (yellow solid lines). b) Cone angles experienced by the triptycene C–D bonds at the α-positions (blue) and β-positions (red). Simulated ^{2}H NMR spectra for (c) the α-C–D bonds at all exchange frequencies and (d) the β-C–D bonds assuming a 3-fold symmetric rotation: 120° jump (above) and 30° jump (below). (e) Representation of the molecular rotation for 3-fold 120° jump (above) and 3-fold 30° jump (below).

is separate and shows almost no interaction with any other pentiptycene. This result indicates that the bulky concave NHC ligand can be expected to prevent strong stacking between pentiptycene units (Figure S11 and S12). The distances between the rotators and the phenyl groups of the stators are shown in Figure 3c. For rotor **2a**, some phenylene groups are very close to the pentiptycene moieties (indicated in pink). The distance of those phenylene groups from the center of triptycene is 4.18 Å, and the shortest distance between a phenylene and the pentiptycene is 3.54 Å. In fact, these two phenylene groups are able to prevent the dynamic motion of pentiptycene because they are located in the path of rotation. The molecular geometry of rotor **2b** is different from that of rotor **2a**. The shortest distance from the rotator to a neighboring phenylene is 3.68 Å (Figure 3c), indicating that the steric hinderance between the phenylene of the stator and rotator in **2b** should be less than that in **2a**. The steric environment near the rotators is shown in Figure 3d. For rotor **2a**, two phenyl rings of the NHC ligand of the same molecule as the rotator and two additional phenyl groups from neighboring molecules are close to the rotator; these are shown in pink and purple, respectively. The shortest distances between the carbon atoms of those units and the rotational center of the pentiptycene are 7.03 Å (purple phenyl groups) and 4.18 Å (pink phenyl groups). The distance between the purple phenyl groups and the rotational center is slightly longer than the rotational radius of the pentiptycene rotator (6.50 Å), while the distances between the meta carbon atoms of the two phenyl rings colored in pink and the rotational center is shorter than the radius of the pentiptycene rotator. It should be noted here that the geometry of the phenyl groups near rotor **2a** can be expected to be able to assume different rotational conformations, which may allow the pentiptycene in **2a** to exhibit rotational motion (for details, see the Supporting Information, Figure S8 and S9). On the other hand, a distinct packing environment was found for rotor **2b**. The distance between the phenylene moieties of the adjacent molecules colored in purple and the rotational center (4.31 Å) is shorter than the rotational radius of pentiptycene. This steric environment around the pentiptycene would prevent its rotational motion in the crystal. Moreover, the orientation of the phenyl rings near rotor **2b** would preclude its rotation, because the rotation axis of the phenyl moiety is vertical to the rotation axis of **2b**, which should suppress the motion of rotor **2b**. Based on the crystal-structure analysis, we assumed that the crystal of giant rotor **2** would exhibit two different molecular motions corresponding to **2a** and **2b**. The packing structure of rotor **2** in the non-solvated crystal was maintained during varying the temperature range in 233 K–353 K, determined by the variable temperature PXRD measurement and DSC study (Figure S3b and S6)

To investigate the molecular motion of crystalline rotors **1** and **2**, we carried out variable-temperature (VT) solid-state (SS) ^{2}H NMR spin-echo measurements with line shape simulations. This method is ideally suited for determining the dynamics of deuterium-enriched moieties with site-exchange rates in the dynamic range of ca. 10^3–10^7 s^{-1}.[32] The key parameters for the rotation of the aromatic groups are the cone angles between the C–D bonds and the rotation axis. For rotor **1**, two different

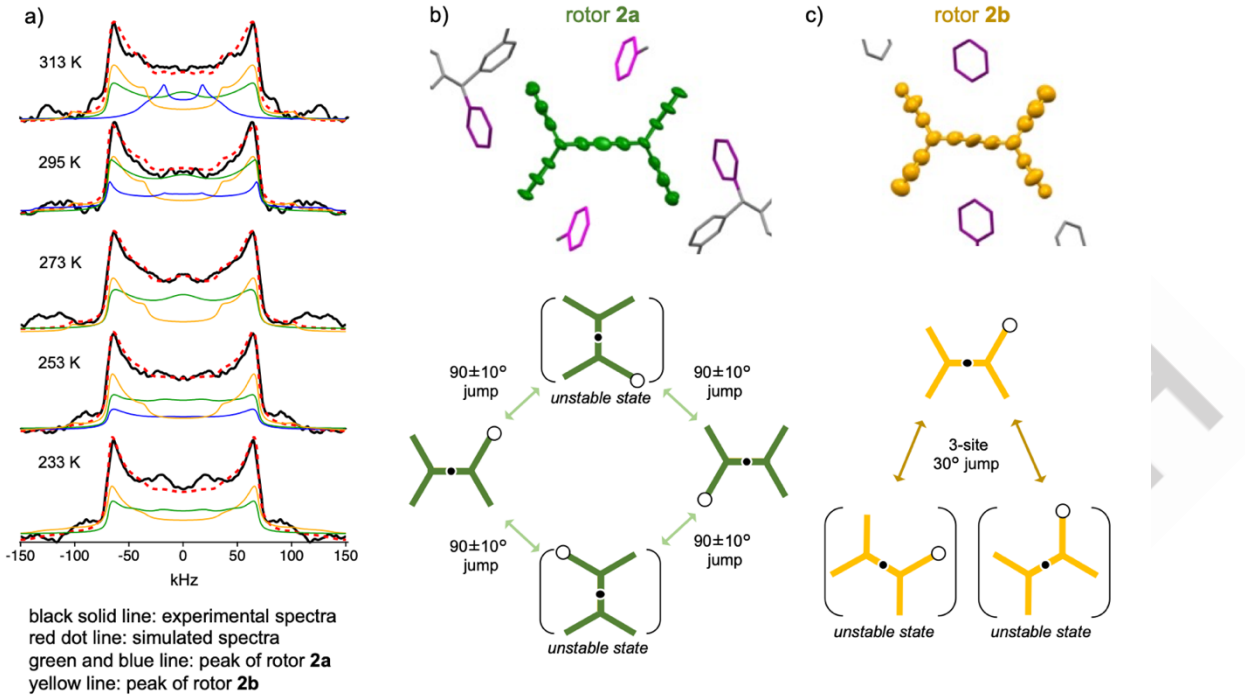

Figure 5. a) Various temperature (VT) solid-state (SS) ^{2}H NMR studies of rotor **2** in crystal **2**. Experimental SS NMR spectra (solid black lines) and simulated spectra: superposition of all simulated spectra (red dashed lines), and simulated spectra for rotor **2a** (green and blue solid lines) and rotor **2b** (yellow solid lines). Packing environment around the rotators and representation of the molecular rotation for b) rotor **2a** and c) rotor **2b**.

deuterium atoms would contribute to the ^{2}H NMR spectrum: the deuterium atoms at the α-carbon (cone angle = 0°) and the β-carbon (cone angle = 60°). The deuterium atoms at the α-carbon would not be expected to exhibit any line-shape change upon molecular rotation, and gave rise to a Pake pattern with two shoulders. In contrast, the ^{2}H NMR signal from the deuterium atoms at the β-carbon exhibited a molecular-motion-dependent line-shape change. In the VT ^{2}H NMR measurements of rotor **1** in the desovlated crystalline sample, clear changes in the line shape were observed during the heating process from 295 to 348 K (Figure 4a and S13a). Based on the line-shape simulations, the dynamics of triptycene seem to have a multi-component mode of motion with 3-fold 120° Brownian jumping and 3-site 30° jumping. The simulated rotational frequencies (k_{rot}) for the 3-fold 120° jumping were 300, 600, 900, 1200, and 1800 kHz at 273, 295, 313, 333, and 348 K, respectively (Figure S14 and S15). Arrhenius plots were constructed based on the rotational exchange frequencies observed at each of the experimental temperatures for rotor **1** (Figure S16). The activation energy (E_a) for rotor **1** was 4.3 kcal/mol, and the preexponential factor (k_0) was calculated to be 9.1 × 10^8 s^{-1}, which is three orders of magnitude smaller than the theoretically expected one (5.6 × 10^{11} s^{-1}).[27,28] The smaller experimentally obtained k_0 value can be rationalized in terms of a correlated motion with the neighboring phenyl rings.[14] Although it is hard to accurately compare the rotational behavior between previously reported triptycene rotors and **1** due to potential effects that may arise from the distinct chemical composition, we noted that the central triptycene in crystal **1** exhibits faster rotation with a lower E_a than that of a triptycene rotor with a convex stator.[27] This result suggests that the encapsulation strategy based on the concave NHC stator may efficiently facilitate the rotation of a bulky rotator in the solid state, e.g., in MOFs.[28]

The spectra obtained for giant rotor **2** also exhibited clear line-shape changes, especially around –50 to 50 kHz from 233 to 313 K, indicating that molecular motion of pentiptycene occurred in the solid state (Figure 5 and S13b). The line-shape simulations for the spectra of giant rotor **2** took into account the fact that the two crystallographically independent pentiptycenes (**2a** and **2b**) are located in different packing environments (Figure 5b). The simulation patterns of rotor **2a** assumed 2-fold site exchanges and applied different population-site ratios (Table 1). At lower temperatures, rotor **2a** showed 2-fold 100° and/or 2-fold 80° jumping at k_{rot} values of 100–150 kHz. These 2-fold motions became 2-fold 90° jumping motions at 273 K, and finally, 4-fold 90° jumping motions combined with 2-fold 90° jumping at 295 and 313 K, with k_{rot} values of 260 and 400 kHz, respectively (Figure 5b and S17–S18). Rotor **2b** cannot fully rotate due to the strongly stacked phenylene, but showed small-angle motion such as libration. The line-shape simulation suggested that a 3-site 30° jump occurred from 233 to 313 K for rotor **2b** with a k_{rot} value of 300-1200 kHz (Figure 5b and S19). It should also be noted here that owing to the unique structure concave spaces, multiple metastable states can be expected to exist in the crystal, resulting in site exchange with different populations. These factors should make it difficult to predict the molecular motion of **2a** in the solid state, and therefore, we cannot dismiss the possibility of other molecular motions. However, the clear line-shape change in the NMR spectra indicates that molecular motion of pentiptycene occurs in the solid state. An Arrhenius plot for rotor **2** could not be prepared due to the different motions that occur at each temperature.

Table 1. Simulated rotational motions and their frequency (k_{rot}) for rotors **2a** and **2b** at various temperatures.

	rotor **2a**			rotor **2b**	
T [K]	green line	blue line	k_{rot} [kHz]	yellow line	k_{rot} [kHz]
313	2-fold 90° (0.8)[a]	4-fold 90° (0.2)[a]	400	3-site, 30°	1200
295	2-fold 90° (0.7)[a]	4-fold 90° (0.3)[a]	260	3-site, 30°	950
273	2-fold 90°	—	200	3-site, 30°	800
253	2-fold 100° (0.8)[a]	2-fold 80° (0.2)[a]	150	3-site, 30°	500
233	2-fold 100°	—	100	3-site, 30°	300

[a]: indicating contribution weight of the motions.

Conclusion

Here, we have described the first example of crystalline materials in which bulky iptycene derivatives (triptycene for **1**, pentiptycene for **2**) exhibit rotational dynamics in the solid state. Single-crystal X-ray diffraction measurements revealed that encapsulation by a large concave NHC ligand provides reasonable rotational space around the central rotator, whereby the formation of intermolecular interactions between the rotators and nearby moieties is suppressed. Variable-temperature ^{2}H solid-state NMR studies suggested that multiple molecular motions occur in both bulky rotors between 233 K and 348 K. These results strongly indicate that this platform will enable further study and design of systems in which large and complicated molecular units exhibit rotational motion while retaining high levels of structural integrity and mobility of the molecular components, and greatly enhance the development of new functional materials based on the dynamics of large molecules in crystalline solids.

Acknowledgements

This work was financially supported by the Japan Society for the Promotion of Science (JSPS) via KAKENHI grants JP17H06370, JP17H06372, JP21K14637, JP22K18333, and JP22H00318; by the JST via CREST grant JPMJCR19R1; by the JSPS Fellows JP22J20934 and JP22KJ0116; and by the Institute for Chemical Reaction Design and Discovery (ICReDD), established by the World Premier International Research Initiative (WPI), MEXT, Japan. The XRD data using synchrotron source were collected at the beamline AR-NW12A of Photon Factory, KEK, Japan (PF-PAC Proposal number: 2022G592).

Keywords: Molecular Rotors; Crystalline Materials; N-Heterocyclic Carbenes; Gold Complex

[1] K. Kinbara, T. Aida, *Chem. Rev.* **2005**, *105*, 1377–1400.
[2] J. P. Morth, B. P. Pedersen, M. J. Buch-Pedersen, J. P. Andersen, B. Vilsen, M. G. Palmgren, P. Nissen, *Nat. Rev. Mol. Cell Biol.* **2011**, *12*, 60–70.
[3] H. Saibil, *Nat. Rev. Mol. Cell Biol.* **2013**, *14*, 630–642.
[4] Kinbara, K.; Howard, J.; Hudspeth, A. J.; Vale, R. D. *Nature* **1989**, *342*, 154–158.
[5] Olesen, C.; Picard, M.; Winther, A.-M. L.; Gyrup, C.; Morth, J. P.; Oxvig, C.; Møller, J. V.; Nissen, P. *Nature* **2007**, *450*, 1036–1042.
[6] Chong, J. H.; MacLachlan, M. J. *Chem. Soc. Rev.* **2009**, *38*, 3301–3315.
[7] Jiang, Y.; Chen, C.-F. *European J. Org. Chem.* **2011**, *2011*, 6377–6403.
[8] Chiu, C.; Yang, J. *ChemPhotoChem* **2020**, *4*, 538–563.
[9] Vogelsberg, C. S.; Garcia-Garibay, M. A. *Chem. Soc. Rev.* **2012**, *41*, 1892–1910.
[10] A. Comotti, S. Bracco, P. Sozzani, *Acc. Chem. Res.* **2016**, *49*, 1701–1710.
[11] Catalano, L.; Naumov, P. *CrystEngComm* **2018**, *20*, 5872–5883.
[12] Gonzalez-Nelson, A.; Coudert, F. X.; van der Veen, M. A. *Nanomaterials* **2019**, *9*, 330.
[13] Howe, M. E.; Garcia-Garibay, M. A. *J. Org. Chem.* **2019**, *84*, 9835–9849.
[14] Liepuoniute, I.; Jellen, M. J.; Garcia-Garibay, M. A.. *Chem. Sci.* **2020**, *11*, 12994–13007.
[15] Ehnbom, A.; Gladysz, J. A. *Chem. Rev.* **2021**, *121*, 3701–3750.
[16] Dong, J.; Wee, V.; Peh, S. B.; Zhao, D. *Angew. Chem., Int. Ed.* **2021**. *60* , 16279-16292.
[17] Akutagawa, T.; Koshinaka, H.; Sato, D.; Takeda, S.; Noro, S.-I.; Takahashi, H.; Kumai, R.; Tokura, Y.; Nakamura, T. *Nat. Mater.* **2009**, *8*, 342–347.
[18] Bureekaew, S.; Horike, S.; Higuchi, M.; Mizuno, M.; Kawamura, T.; Tanaka, D.; Yanai, N.; Kitagawa, S. *Nat. Mater.* **2009**, *8*, 831–836.
[19] W. Setaka, K. Yamaguchi, *J. Am. Chem. Soc.* **2012**, *134*, 12458–12461.
[20] N. B. Shustova, T.-C. Ong, A. F. Cozzolino, V. K. Michaelis, R. G. Griffin, M. Dincă, *J. Am. Chem. Soc.* **2012**, *134*, 15061–15070.
[21] W. Setaka, K. Yamaguchi, *J. Am. Chem. Soc.* **2013**, *135*, 14560–14563.
[12] Harada, J.; Ohtani, M.; Takahashi, Y.; Inabe, T. *J. Am. Chem. Soc.* **2015**, *137*, 4477–4486.
[23] Jin, M.; Chung, T. S.; Seki, T.; Ito, H.; Garcia-Garibay, M. A. *J. Am. Chem. Soc.* **2017**, *139*, 18115–18121.
[24] Jin, M.; Yamamoto, S.; Seki, T.; Ito, H.; Garcia-Garibay, M. A. *Angew. Chem., Int. Ed.* **2019**, *58*, 18003–18010.
[25] Colin-Molina, A.; Karothu, D. P.; Jellen, M. J.; Toscano, R. A.; Garcia-Garibay, M. A.; Naumov, P.; Rodríguez-Molina, B. *Matter* **2019**, *1*, 1033–1046.
[26] Yao, Z.-S.; Guan, H.; Shiota, Y.; He, C.-T.; Wang, X.-L.; Wu, S.-Q.; Zheng, X.; Su, S.-Q.; Yoshizawa, K.; Kong, X.; Sato, O.; Tao, J. *Nat. Commun.* **2019**, *10*, 4805.
[27] Jiang, X.; Rodríguez-Molina, B.; Nazarian, N.; Garcia-Garibay, M. A. *J. Am. Chem. Soc.* **2014**, *136*, 8871–8874.
[28] Jiang, X.; Duan, H.-B.; Khan, S. I.; Garcia-Garibay, M. A. *ACS Cent Sci* **2016**, *2*, 608–613.
[29] Jin, M.; Ando, R.; Jellen, M. J.; Garcia-Garibay, M. A.; Ito, H. *J. Am. Chem. Soc.* **2021**, *143*, 1144–1153.
[30] Jin, M.; Matsuura, S.; Yamamoto, H.; Mizuno, M.; Ito, H. *European J. Org. Chem.* **2023**. *26*, e202201468.

[31] Zhao, Q.; Meng, G.; Li, G.; Flach, C.; Mendelsohn, R.; Lalancette, R.; Szostak, R.; Szostak, M. *Chem. Sci.* **2021**, *12*, 10583–10589.

[32] Macho, V.; Brombacher, L.; Spiess, H. W. The NMR-WEBLAB: An Internet Approach to NMR Lineshape Analysis. *Appl. Magn. Reson.* **2001**, *20*, 405–432.

[33] Deposition numbers 2259660 (for $\mathbf{1}_{sol}$), 2259662 (for **2**), and 2259661 (for $\mathbf{2}_{sol}$) contain the supplementary crystallographic data for this paper. These data are provided free of charge by the joint Cambridge Crystallographic Data Centre and Fachinformationszentrum Karlsruhe Access Structures service.

Entry for the Table of Contents

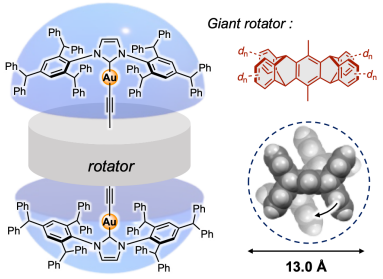

Here, we have described the first example of crystalline materials in which bulky iptycene derivatives (triptycene and pentiptycene) exhibit rotational dynamics in the solid state. It is revealed that encapsulation by a large concave NHC ligand provides reasonable rotational space around the central rotator. This platform will enable further design of systems in which large and complicated molecular units exhibit rotational motion in solid.

Institute and/or researcher Twitter usernames: @MingooJin, @haj19932469, @ICReDDconnect (Twitter)